Jpn. J. Appl. Phys. Vol. 39 (2000) pp. 6264–6267
Part 1, No. 11, November 2000

Output Characteristics of P-doped Raman Fiber Laser at 1484 nm with 2.11 W Maximum Output Power Pumped by CW 1064 nm Yb-doped Double-Clad Fiber Laser

Nam Seong KIM[1,2,*], Mahendra PRABHU[1], Cheng LI[1], Jie SONG[1] and Ken-ichi UEDA[1]

[1]*Institute for Laser Science, Univ. of Electro-Communications, 1-5-1 Chofugaoka, Chofu, Tokyo 182-8585, Japan*
[2]*Information and Telecommunications Technology Center, The University of Kansas, Lawrence, Kansas 66047, U.S.A.*

(Received March 6, 2000; accepted for publication June 19, 2000)

The output dependence on output reflectivity and fiber length is reported for a phosphosilicate Raman fiber laser (RFL) at the second Stokes wavelength of 1484 nm using a pump of CW 8.4 W/1064 nm Yb-doped double-clad fiber laser (DCFL) and cascaded cavities for the first and second Stokes wavelength. The output reflectivities for the second Stokes light were 15 and 50% and the lengths of the P-doped Raman fiber (PDF) were 300, 700, and 1000 m. The maximum output of 2.11 W/1484 nm was obtained using 15% output reflectivity and 700 m PDF length and the corresponding slope efficiency from the pump was 33.2%. The laser performance for the six configurations was investigated by observing the maximum output power, slope efficiency, threshold pump power, and full-width at half maximum at the second Stokes wavelength.

KEYWORDS: fiber laser, Raman laser, Raman fiber amplifiers, optical amplifiers, optical fiber communications

1. Introduction

Since the late 1990s, Raman fiber amplifiers (RFAs) and lasers (RFLs) have been actively studied by several groups.[1–10] The major applications for RFLs are as high-power pumping sources for 1310 and 1550 nm fiber amplifiers in optical fiber communications using 1240 and 1480 nm wavelengths, respectively. The RFL at 1240 nm is the only pump source with very low loss for 1310 nm Raman fiber amplifiers since there are very few commercial laser diode (LD) sources at this wavelength. The RFL at 1480 nm is also a good alternative for pumping Er-doped fiber amplifiers since the available LD sources at this wavelength have only 100 to 200 mW output power and are more expensive than the high-power, over 1 W RFL. Active research during the late 1990s resulted in the fast development of the Yb-doped Double-clad fiber laser (DCFL)[11–13] which has an output power of 20 to 50 W at any wavelength from 1040 to 1120 nm and is a very efficient pumping source for RFLs at 1240 and 1480 nm. Two methods have been developed for the 1240 nm and 1480 nm RFLs. One method uses a Ge-doped fiber (GDF),[14] which has peak Raman shift of 430 cm^{-1}. When we use a strong 1060 nm pump for the GDF, the RFLs at 1240 and 1480 nm are the third and the sixth Stokes which require complicated three and six cascaded cavities, respectively. However, the GDF's wide gain bandwidth allows wide wavelength selectivity. The other method uses a P-doped fiber (PDF),[15–20] which has a peak Raman shift of 1330 cm^{-1}. When we use a strong 1060 nm pump for the PDF, the RFLs at 1240 and 1480 nm are the first and the second Stokes which require simple one and two cascaded cavities, respectively. However, the PDF's narrow gain bandwidth does not allow wavelength selectivity. However, if a 1120 nm Yb-doped DCFL and the GDF at the first stage is used, the PDF at the second stage can give wide wavelength selectivity at the 1480 nm band using only three cascaded cavities for 1180–1240–1480 nm chain which is half the number required for the GDF-only RFL at 1480 nm.

However, there are only a few reports on the RFL using the PDF and additionally the output characteristics of such RFLs have not been examined in detail.[2)] Therefore, in this paper, detailed output characteristics are reported for the RFL at 1484 nm using the PDF, CW 8.4 W Yb-doped DCFL as a pumping source, and the cascaded 1239 and 1484 nm cavities. By using three PDF lengths of 300, 700, and 1000 m and output reflectivities of 15% and 50%, the dependences on the length and reflectivity are investigated. The maximum output power, slope efficiency, threshold pump power and full-width at half maximum (FWHM) at 1484 nm are measured for the six configurations. Based on the former experimental results[19)] and separate simulation, it was believed that the 1000 m fiber length was overly long since the fiber loss at 1484 nm was larger than the Raman gain from the initial pump at this length. The simulation showed that the maximum output power can be obtained for a fiber length between 600 and 800 m for various configurations. Therefore, the medium fiber length of 700 m was chosen in this experiment to attempt to obtain a maximum output power. The fiber Bragg grating (FBG) output reflectivity of 15% was selected after considering the difficulty in FBG fabrication even though a maximum output power was expected from an output reflectivity lower than 15% based on a simulation. The combination of 15% output reflectivity and 700 m PDF length generated the output power of 2.11 W and the slope efficiency of 33.2%, which is the highest output which has been officially reported thus far, to the best of our knowledge. On observing the residual pump power (RPP), there is a three-step change that is explained as the power-transfer processes from the pump to the first-Stokes and from the first-Stokes to the second Stokes. The first Stokes power at the output fiber is almost constant after the second Stokes output is created. The fiber length of 700 m resulted in the highest output power and the lowest threshold pump power. The RFL using a 1000 m PDF length generated an asymmetric spectral profile with a stable shoulder, which may be the result of nonlinear interaction.

2. Experiments

Figure 1 shows the setup for the 1484 nm RFL experiments. The pumping source was a Yb-doped DCFL with CW 8.4 W/1064 nm single-mode output and its output pigtail was a Flexcor-1060 single-mode fiber (SMF) with a core diameter of 6 μm, manufactured by Corning. The FBG mirrors for the first and second Stokes cavities were fabricated on the

*Present address: Qtera division of Nortel Networks, 6800 Broken Sound Parkway N.W., Boca Raton, Florida 33487, U.S.A.

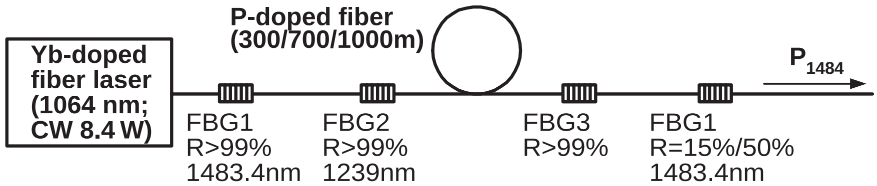

Fig. 1. Experimental setup of the 1484 nm Raman fiber laser pumped by a CW 8.4 W/1064 nm Yb-doped double-clad fiber laser.

Flexcor-1060 SMF using an excimer laser. The reflectivities of the FBG mirrors were more than 99% for both full mirrors at 1239 and 1484 nm. For the output mirror at 1484 nm, two types of 15 and 50% reflectivities were used. Therefore, very high conversion from 1239 to 1484 nm wavelengths could be achieved. A low splicing loss could be achieved since the fibers for the DCFL output and the FBG were identical and the 6 μm mode-field diameter of the PDF was also similar to that of the Flexcor-1060. The Raman gain medium was a P-doped single-mode optical fiber fabricated by the General Physics Institute. Fiber lengths of 300, 700, and 1000 m were used. The PDF had 12 mol% of P_2O_5 and the refractive index difference was 0.0107. The loss of the PDF was 1.84, 1.23, and 1.00 dB/km at 1064, 1239, and 1484 nm, respectively. The mode-field diameter of the PDF was 5.96, 7.05, and 8.25 μm at 1064, 1239, and 1484 nm, respectively. The output spectrum was measured using a AQ-6315B optical spectrum analyzer (ANDO Co.). The output power was measured using a LaserMate optical power meter (Coherent Inc.). Since the fiber laser output was too large to input to the optical spectrum analyzer, a small part of the output was launched into a graded-index (GRIN) lens with a FC/PC optical connector which was connected to the optical spectrum analyzer to measure the relative power ratio among the 1064, 1239, and 1484 nm spectral pulses. A 0.05 nm spectral resolution and 10 nm span were used to measure each relative optical power. Then, the absolute output power of each spectral component was calibrated using the absolute output power measured using the LaserMate optical power meter.

The spectral profiles for the RFL output are shown in Fig. 2, which used a 50% output reflectivity and 300, 700, and 1000 m PDF lengths for (a), (b), and (c), respectively. For the combinations, the spectral profiles in Fig. 2 are for the maximum output powers of 1.00, 1.64, and 1.30 W for (a), (b), and (c), respectively. Their peaks were normalized in order to allow comparison of the FWHMs which were 0.75, 2.14, and 1.87 nm for 300, 700, and 1000 m PDF lengths, respectively. For the 1000 m PDF length, a flat shoulder near 1483.1 nm is shown which is slightly shorter wavelength than the main peak wavelength of 1483.7 nm and is thought to be a result of increased nonlinear interactions in longer fiber lengths. Figure 3 shows the output powers of the residual pump, the first Stokes, and the second Stokes lights with the change of input pump power. It is the case of 15% output reflectivity at the second Stokes wavelength and 700 m PDF length, which gives us the highest output power of 2.11 W in this experiment. To the best of our knowledge, the output power of 2.11 W is the largest one reported for the P-doped Raman fiber laser. Threshold pump powers are 0.60 and 1.82 W for the first and second Stokes lights, respectively, and the slope efficiency is 33.2%. The inset of Fig. 3 is for the 700 m PDF

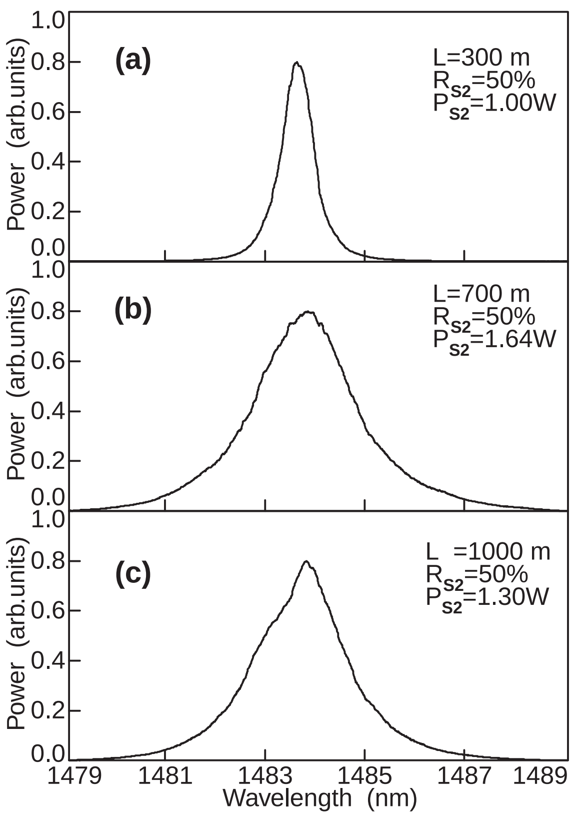

Fig. 2. Spectral profiles for the RFL output for a 50% output reflectivity and 300, 700, and 1000 m PDF lengths for (a), (b), and (c), respectively.

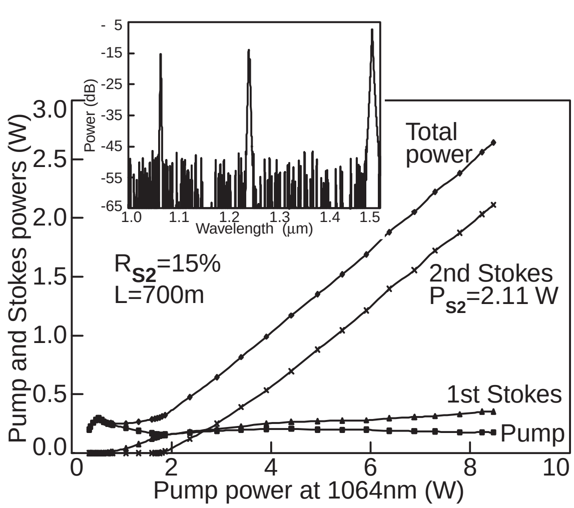

Fig. 3. Evolution of the output powers for the residual pump, the first Stokes, and the second Stokes lights with the change of input pump power. Inset: output spectrum at 2.11 W second Stokes power.

length and 15% FBG output reflectivity and the vertical scale is logarithmic. It is shown that the pump and the first Stokes levels are about 9 dB lower than the second Stokes level. The noise level is 40 dB lower than that at the 1484 nm wavelength. The three-step change for the residual pump power is clearly observed. In the first step, the residual pump power is proportional to the input pump power since it undergoes only total cavity loss before generating the first and the second Stokes lights. In the second step, the residual pump power is inversely proportional to the input pump one since major power is converted to the first Stokes one after generation of the first Stokes light. This indicates that more than the pure increase amount of the input pump power is converted to the first Stokes power. In the third step, the first Stokes power is transferred to the second Stokes one after generation of the second Stokes light. In this case, the residual pump power is still decreasing, but the rate of decrease becomes slower than the second step since more than the pure increase amount of the input pump power is still converted to the first Stokes power. When part of the pure increase amount of the input pump power is converted to the first Stokes power, the residual pump power is increased with a slow rate; this was confirmed for the 15% output reflectivity and the 300 m PDF length. Fluctuation of the output power at 1484 nm was less than 2% during short-term observation.

Figure 4 shows the second Stokes power with the change of the PDF length. For the 300 m PDF length, the second Stokes power was about 1.00 W for both the 15 and 50% output reflectivities at 1484 nm. For the 700 m PDF length, the second Stokes power was the highest among the three PDF lengths of 300, 700, and 1000 m. It was 2.11 and 1.64 W for 15 and 50% output reflectivities, respectively. For the 1000 m PDF length, the second Stokes power was middle among the three lengths. Therefore, all combinations generated more than 1 W for the second Stokes power and more than 2 W was generated for the combination of 15% output reflectivity and 700 m PDF length. The slope efficiency from the input pump to the second Stokes power is shown in Fig. 5. It is proportional to the second Stokes power, but there is a slight difference since the threshold pump power is different for each combination. The total slope efficiency is for the total input pump power. The net slope efficiency is for the convertible input pump power which excludes the nonconversion loss due to splicing loss, total cavity loss for the FBG mirrors, and the residual pump power from the input pump power, and can be converted to the second Stokes power through the first Stokes one. The net slope efficiency is the measure of the system performance and indicates how much the slope efficiency can be improved if we reduce the nonconversion loss. The total slope efficiencies are 21.7/33.2/27.6% for 300/700/1000 m for the 15% output reflectivity and 17.8/24.1/19.4% for 300/700/1000 m for the 50% one. The net slope efficiencies are 32.5/56.3/58.0% for 300/700/1000 m for the 15% output reflectivity and 26.4/44.5/46.7% for 300/700/1000 m for the 50% one. Therefore, we know that the net slope efficiency is proportional to the PDF length when we ignore the total cavity loss. Figure 6 shows the threshold input pump power for generating the second Stokes light with the change of the PDF length and the 700 m PDF length resulted in the lowest threshold input pump power. For the 15% output reflectivity at 1484 nm, the threshold power was 3.84, 1.82, and 2.10 W for 300, 700, and 1000 m, respectively. For the 50% output reflectivity at 1484 nm, the threshold power was 2.73, 1.31, and 1.83 W for 300, 700, and 1000 m, respectively. Since the second Stokes power in the cavity is proportional to the output reflectivity, the Raman gain is increased with the output reflectivity and the threshold power is believed to increase with the output reflectivity. The FWHM is shown in Fig. 7 with the change of the PDF length. The largest FWHM was 2.14 nm for the 50% output reflectivity and 700 m PDF length and is roughly proportional to the second Stokes power.

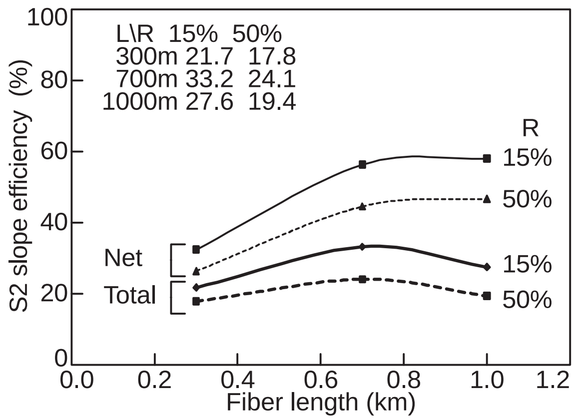

Fig. 5. Slope efficiency of the second Stokes power with the PDF length and the output reflectivity.

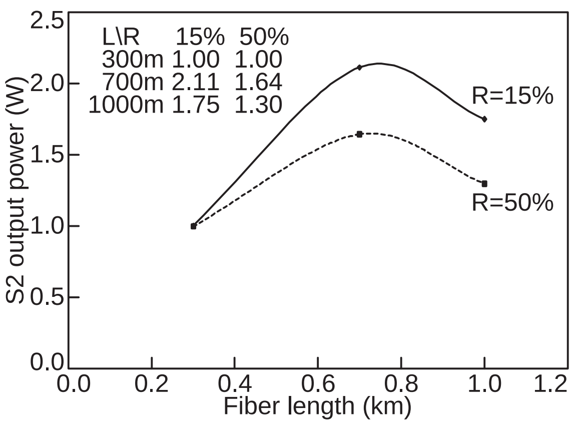

Fig. 4. Second Stokes power with the PDF length and the output reflectivity.

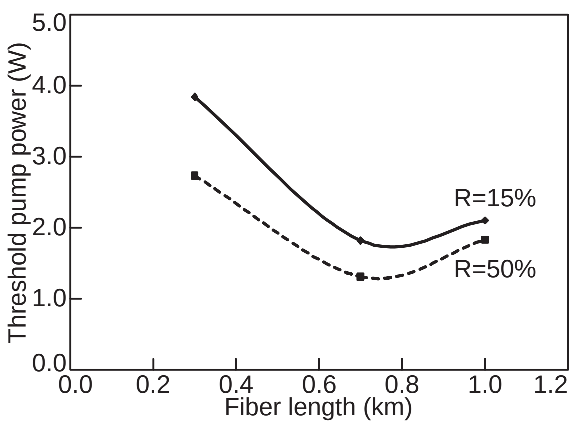

Fig. 6. Threshold input pump power to generate the second Stokes power with the PDF length and the output reflectivity.

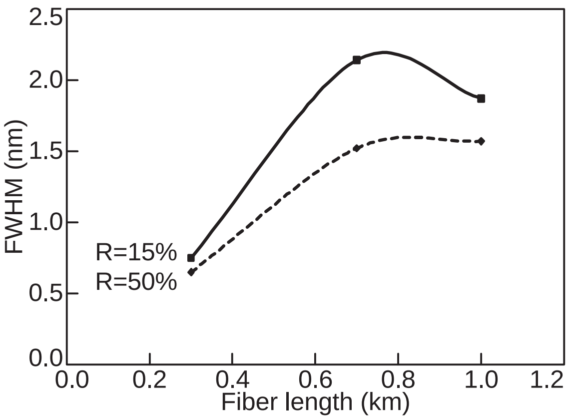

Fig. 7. FWHM of the second Stokes power with the PDF length and the output reflectivity.

3. Conclusions

In conclusion, we investigated the output characteristics for the Raman fiber laser at 1484 nm using a PDF, 1064 nm Yb-doped DCFL, and two cascaded FBG-mirror pairs for the first and the second Stokes lights. The used output reflectivities at 1484 nm were 15% and 50% and the used PDF lengths were 300, 700, and 1000 m. The maximum output power at 1484 nm was 2.11 W using the 15% output reflectivity and 700 m PDF length and this is the maximum power reported for the PDF Raman fiber laser at 1484 nm. For the six configurations of different lengths and reflectivities, we investigated the second Stokes power, slope efficiency, threshold input pump power, and FWHM. The 1484 nm Raman fiber laser with a 2 nm FWHM and more than 2 W power will be very useful as a pumping source of Er-doped fiber amplifiers in optical fiber communications and it can also be applied to very broad-band Raman fiber amplifiers when the output wavelength is changed by varying the initial pump wavelength.

1) H. Masuda and S. Kawai: IEEE Photon. Technol. Lett. **11** (1999) 647.
2) E. M. Dianov: Proc. 10th Optical Amplifiers and their Applications Conf., Nara, Japan, 1999, ThA2-1 (1999) p. 70.
3) S. A. E. Lewis. S. V. Chernikov and J. R. Taylor: Electron. Lett. **35** (1999) 1178.
4) D. Hamoir, D. Bayart, J. Boniort and C. L. Sergent: Proc. 10th Optical Amplifiers and their Applications Conf., Nara, Japan (1999).
5) J. Kani, M. Jinno and K. Oguchi: Electron. Lett. **34** (1998) 1745.
6) H. Masuda, S. Kawai, K. Suzuki and K. Aida: IEEE Photon. Technol. Lett. **10** (1998) 516.
7) H. Masuda, S. Kawai, K. Suzuki and K. Aida: Electron. Lett. **34** (1998) 2339.
8) H. Masuda, S. Kawai and K. Aida: Electron. Lett. **34** (1998) 1342.
9) A. Bertoni and G. C. Reali: Appl. Phys. B **67** (1998) 5.
10) P. B. Hansen, L. Eskildsen, S. G. Grubb, A. J. Stentz, T. A. Strasser, J. Judkins, J. J. DeMarco, R. Pedrazzani and D. J. DiGiovanni: IEEE Photon. Technol. Lett. **9** (1997) 262.
11) M. Muendel, B. Engstrom, D. Kea, B. Laliberte, R. Minns, R. Robinson, B. Rockney, Y. Zhang, R. Collins, P. Gavrilovic and A. Rowley: CLEO'97, Baltimore, May 18–23, 1997, postdeadline papers CPD (1997) p. 30.
12) A. S. Kurkov, O. I. Medvedkov, V. I. Karpov, S. A. Vasiliev, O. A. Lexin and E. M. Dianov: OFC'99, San Diego, Feb. 21–26, 1999, WM4.
13) V. Dominic, S. MacCormack, R. Waarts, S. Sanders, S. Bicknese, R. Dohle, E. Wolak and E. Zucker: Electron. Lett. **35** (1999) 1158.
14) A. J. Stentz: Proc. SPIE **3263** (1998) 91.
15) V. I. Karpov, E. M. Dianov, V. M. Paramonov, M. M. Bubnov, S. L. Semyonov, S. A. Vasiliev, V. N. Protopopov, O. N. Egorova, V. F. Hopin, A. N. Guryanov, M. P. Bachynski and W. R. L. Clements: Opt. Lett. **24** (1999) 887.
16) V. I. Karpov, E. M. Dianov, A. S. Kurkov, V. M. Paramonov, V. N. Protopopov, M. P. Bachynski and W. R. L. Clements: OFC'99, San Diego, Feb. 21–26, 1999, WM3.
17) E. M. Dianov, M. V. Grekov, I. A. Bufetov, V. M. Mashinsky, O. D. Sazhin, A. M. Prokhorov, G. G. Devyatykh, A. N. Guryanov and V. F. Khopin: Electron. Lett. **34** (1998) 669.
18) E. M. Dianov, M. V. Grekov, I. A. Bufetov, S. A. Vasiliev, O. I. Medvedkov, V. G. Plotnichenko, V. V. Koltashev, A. V. Belov, M. M. Bubnov, S. L. Semyonov and A. M. Porkhorov: Electron. Lett. **33** (1997) 1542.
19) N. S. Kim, M. Prabhu, C. Li, J. Song and K. Ueda: Opt. Commun. **176** (2000) 219.
20) M. Prabhu, N. S. Kim and K. Ueda: to be published in Opt. Rev. (2000).